Am J Cancer Res 2018;8(9):1752-1763
www.ajcr.us /ISSN:2156-6976/ajcr0072031

Original Article

Transglutaminase-2 promotes metastatic and stem-like phenotypes in osteosarcoma

Daniel G Fuja[1,2], Nino C Rainusso[1], Ryan L Shuck[1], Lyazat Kurenbekova[1], Lawrence A Donehower[1,2,3,4,5], Jason T Yustein[1,2,3,5]

[1]Texas Children's Cancer and Hematology Centers and The Faris D. Virani Ewing Sarcoma Center, Baylor College of Medicine, Houston 77030, Texas, USA; [2]Integrative Molecular and Biological Sciences Program, Baylor College of Medicine, Houston 77030, Texas, USA; [3]Department of Molecular and Cellular Biology, Baylor College of Medicine, Houston 77030, Texas, USA; [4]Department of Molecular Virology & Microbiology, Baylor College of Medicine, Houston 77030, Texas, USA; [5]Dan L. Duncan Cancer Center, Baylor College of Medicine, Houston 77030, Texas, USA

Received January 3, 2018; Accepted January 12, 2018; Epub September 1, 2018; Published September 15, 2018

Abstract: Osteosarcoma (OS) is a highly aggressive mesenchymal malignancy and the most common primary bone tumor in the pediatric population. OS frequently presents with or develops distal metastases. Patients with metastatic disease have extremely poor survival rates, thus necessitating improved molecular insights into OS metastatic biology. Utilizing our previously characterized genetically engineered mouse model (GEMM) of metastatic OS, we identified enhanced differential expression of Transglutaminase-2 (TGM2) in metastatic OS. However, the role of TGM2 in sarcoma development and metastatic progression remains largely undefined. To further investigate the role of TGM2 in OS metastasis, we performed both gain- and loss-of-function studies for TGM2 in human and mouse OS cell lines. Our data provide evidence that enhanced expression of TGM2 in metastatic OS contributes to migratory and invasive phenotypes. Besides the effects on metastatic phenotypes, we also observed that TGM2 contributes to OS stem-like properties. In addition, treatment with transglutaminase inhibitors had analogous effects on proliferation and migration to TGM2 knockdown. Finally, *in vivo* xenograft studies demonstrated that TGM2 functionally alters metastatic potential and survival outcome. Together, these data highlight TGM2 as a pro-metastatic factor in OS and a potential avenue for future therapeutic intervention to inhibit metastatic disease.

Keywords: Osteosarcoma, metastasis, transglutaminase, stem cell

Introduction

Osteosarcoma (OS) is the most prevalent primary malignant bone cancer that arises from mesenchymal origins [1-4]. This lineage is evidenced by the prevalence of osteoid-an immature bone matrix deposited by OS. Long-term outcomes have improved over the past several decades for patients with localized OS, with five-year survival rates approaching 70%. However, in patients with evidence of metastatic disease there have been no significant improvements in mortality, with overall survival rates of less than 25% [5-8]. In addition to signifying more aggressive disease, metastatic OS has also been associated with increased chemoresistance [9]. Despite the significant differential survival rates and mounting evidence that distal OS metastases are dissimilar to primary OS, most standard protocols for treating metastatic OS today are essentially the same as those for localized disease [10]. OS treatment typically includes surgical resection and high dose chemotherapy, which frequently includes combinations of methotrexate, doxorubicin, cisplatin and ifosfamide [6, 10-12]. This severe deficiency in tailored treatment options for patients with metastatic disease is secondary to a lack of insights into the molecular mechanisms underlying sarcoma metastasis and identification of viable new therapeutic targets.

We have previously developed and characterized a tissue-specific genetically engineered mouse model (GEMM) of metastatic osteosarcoma in order to perform basic molecular and translational investigations of OS [13]. Using this GEMM, we were able to identify significant differentially-expressed genes within a *de novo*

model of osteosarcoma metastasis. From among these differentially expressed genes, we identified Transglutaminase-2 (TGM2) to be significantly elevated in lung and other distal metastatic OS lesions, compared to the bone tumors at the primary site of tumor development.

Transglutaminase-2 is a multifunctional protein involved in several developmental, tissue-specific and homeostatic processes. TGM2 has undergone extensive clinical investigation as an autoantigen and clinically relevant enzyme in celiac disease [14-16]. TGM2 has recently been associated with metastatic phenotypes for several carcinomas, including ovarian, colorectal, prostate, and breast [17-22]. In many of these carcinomas, TGM2 is particularly notable in enhancing the so-called epithelial-mesenchymal transition (EMT) properties [17, 23]. However, whether similar functions would be present in a mesenchymal-derived sarcoma, such as OS, has not yet been investigated.

Our results from complementary gain- and loss-of-function *in vitro* and *in vivo* studies, along with pharmacological targeting, demonstrate TGM2 has the ability to drive metastatic progression and stem cell-like properties in OS. Overall, our examinations indicate that targeting TGM2 in OS might prove to be viable therapeutic target.

Materials and methods

Cell culture

SaOS2 and LM7 human cell lines were generously donated by Dr. Chris Tsz-Kwong Man (Texas Children's Hospital Cancer & Hematology Centers). HOS and 143B human osteosarcoma cell lines were obtained from ATCC (CRL-1543 and CRL-8303). Primary paired mouse OS lines (CR175, RF891, RF1142) were established from GEMM as previously described [13]. All cells were grown and maintained in a humidified culture incubator at 37°C and 5% CO_2. Unless otherwise noted, primary and established cells were grown in Dulbecco's Modified Eagle Medium (DMEM, Gibco), which was supplemented with 10% FBS (Hyclone) and 1% penicillin/streptomycin (Sigma). This media was also used for puromycin selection, with the only difference being the addition of puromycin (Gibco) to concentrations of either 5 μg/mL or 20 μg/ml. Following initial selection, cells were maintained at lower antibiotic concentrations, typically 1 μg/mL. Established cell lines were authenticated at the MD Anderson Authentication Core (https://www.mdanderson.org/research/research-resources/core-facilities/characterized-cell-line-core-facility.html). Cell lines were continuously tested and maintained free of mycoplasma.

Transfection of siRNA, shRNA, and TGM2 overexpression plasmid

Flexitube siRNA (Qiagen) against TGM2 was introduced to the cell lines using RNAimax lipofectamine according to the manufacturer's standard protocol. Maximal knockdown was typically reached between 48 and 72 hours. Scramble siRNA or siRNA to GFP was concurrently and identically transfected as a negative control. Multiple shRNA clones based on the GIPZ backbone were obtained in-house through the Cell Based Assaying and Screening service (C-BASS) at Baylor College of Medicine. Transfection using Lipofectaimine 2000 was successful using the manufacturer's guidelines. Following transfection and 48 hours normalization period, selection with puromycin was initiated for 48 hours at 20 μg/ml. This was followed by several weeks in puromycin (5 μg/ml) selection media, resulting in an enriched population that was then sorted using fluorescence-activated cell sorting (FACS), retaining the top 10% GFP-expressing population conferred by the GIPZ vector. Cells transfected with blank GIPZ vector were used as a negative control.

Full-length FLAG-tagged human TGM2 constitutive-expression constructs (pENTR1A) were created that resulted in significant full-length TGM2 overexpression. A blank vector lacking the TGM2 gene was used as a negative control. Stable cell lines were established in puromycin (5 μg/ml) selection media. All stable cell lines were maintained in puromycin maintenance media (1 μg/mL) following initial selection.

RNA isolation, cDNA reverse transcription, and qPCR

To extract RNA, tissue was homogenized mechanically in Trizol (Invitrogen/Thermo Fisher Scientific). Cells were lysed in Trizol without

mechanical homogenization. For each, chloroform-extraction was performed, followed by separation of the upper aqueous phase and subsequent precipitation with 100% isopropanol then purified using 75% ethanol. RNA quantification was conducted using standard spectrophotometer and/or nanodrop.

cDNA was created from 500 ng-1 μg of RNA using qscript cDNA supermix (Quanta) standard protocol on a Multigene 60 Thermal Cycler (Labnet). cDNA was used to quantify gene expression via qPCR. qPCR was conducted using Fast SYBR (Life Technologies) or iQ SYBR Green Supermix (Biorad).

Protein isolation and western blot

Whole cell lysate (WCL) was isolated through mechanical disruption on ice in RIPA lysis buffer (supplemented with complete protease and phosphatase inhibitor). Following a 30-minute incubation on ice, cells were centrifuged at 12,000 × g for 15 min. The WCL supernatant was collected and either utilized immediately or stored at -20°C for short-term storage or -80°C if held longer. Protein concentration was quantified using the Pierce BCA colorimetric assay (Thermo Fisher Scientific), reading on a Multiscan plate imager at 550 nM and quantified against known BSA standards. Primary and secondary antibodies used were from Cell Signaling Technologies and Thermo. Antibodies were typically diluted in 5% BSA/TBST.

For western blot protein quantification, equal amounts (actual concentration depending on sample pair) of protein were supplemented with Milli-Q water to a final volume of 25 μl, to which 7.5 μl of LDS sample buffer with 5% beta-mercaptoethanol was added. Samples were boiled at 100°C for 10 minutes, followed by a brief cool-down and then loaded onto a 4-12% bis-tris gradient gel (Thermo Fisher Scientific) and run at ~150 V until appropriate ladder band (SeeBlue Plus2, Thermo Fisher Scientific) separation was achieved. For TGM2 western blots, a positive control of purified TGM2 protein (Sino Biological) was used to gauge appropriate band size. Transfer to nitrocellulose membrane was accomplished via standard protocol (iBlot, Thermo Fisher Scientific). Incubation with antibodies was either in a traditional manner (block 5% BSA 1 hr room temp, PBS-T wash × 3, Primary antibody overnight at 4°C, PBS-T wash × 3, Secondary Antibody at room temperature × 1 hr or overnight at 4°C) or via iBind (Thermo Fisher Scientific) standard protocol for TGM2. Membranes were washed (3 ×) and incubated with Western Lightening ECL (PerkinElmer), then imaged using either Kodak film development or the my ECL imaging system (Thermo Fisher Scientific). Capture settings determined by machine were always kept identical for paired samples. Paired samples were always run side-by-side, next to each other and amount loaded was identical between sample pairs. Blots were incubated with RESTORE stripping buffer (Thermo Fisher Scientific) for 15 minutes and re-probed as described above with Actin as endogenous control to ensure consistency.

Proliferation assay and chemosensitivity

Proliferation was evaluated using a tetrazolium salt-based colorimetric assay (Dojindo, CCK-8), in which colorimetric change is directly proportional to viable cell counts. Briefly, 100 μl of cells were seeded at 4×10^4 cells/mL. An additional 100 μl of drugs/inhibitors or media were added for experimental and control wells, respectively. To ensure uniform seeding in all wells, CCK-8 was immediately added to the wells corresponding with the initial time point (day 0). Plates were read 3 hours following introduction of the CCK-8 substrate. Fresh CCK-8 was introduced to untested triplicate wells for each condition/cell type on each subsequent day/time point.

Transwell migration and invasion assays

Migration and invasion were assessed utilizing the transwell Boyden chamber assay as previously described [13]. Briefly, transwell inserts (Corning) were placed into 24-well plates. For invasion, 100 μl of collagen (10 μg/mL) was introduced to the upper chamber and allowed to cure overnight at 37°C. OS cells which had been serum starved for 24 hours were then introduced to the upper chamber and allowed to migrate for 24 to 36 hours, depending on the cell line and treatment. Following this incubation at 37°C with 5% CO_2, the top side of the upper chambers were gently swabbed with cotton-tipped applicators and the underside was fixed with formalin for 15 minutes, followed by crystal violet staining. After washing and drying, transwells were im-

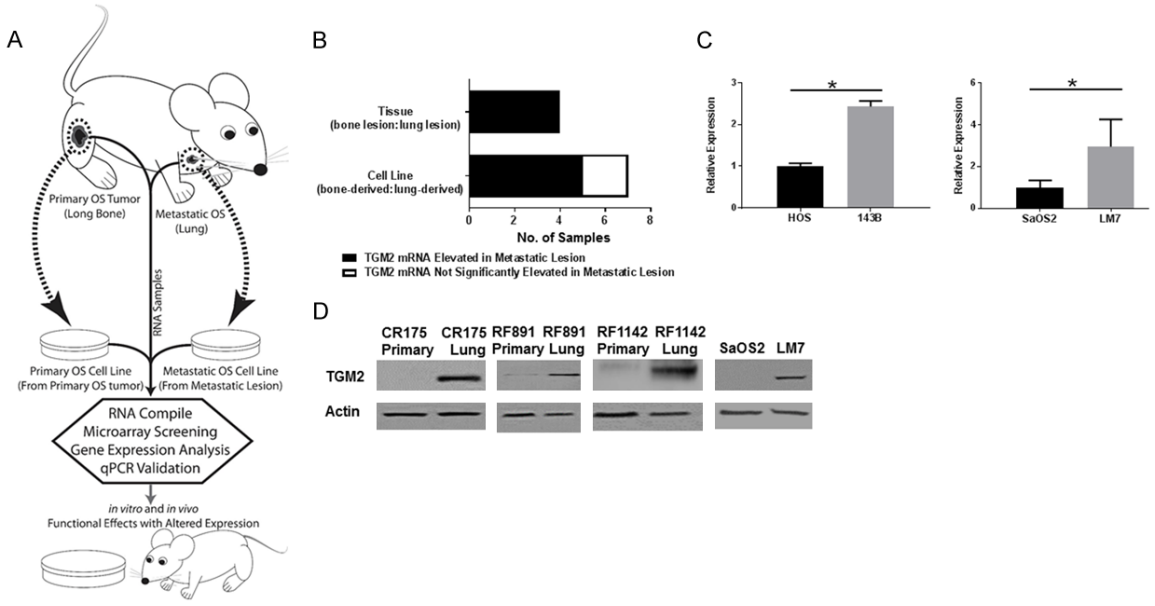

Figure 1. Identification of enhanced TGM2 expression in metastatic OS. A: Schematic demonstrates technical method to compare altered gene expression in primary and metastatic samples of both tissue and corresponding isolated cell lines. B: qPCR validation of number of GEMM sample pairs (Primary vs. metastatic) from individual mouse which demonstrated *Tgm2* upregulation of statistical significance (black fill) or not (empty). C: qPCR of established cell line pairs human OS. 143B and LM7 are metastatic versions of HOS and SaOS2, respectively. D: Western blots from paired GEMM-derived cell lines for TGM2. Right panel is western blot for paired human cell lines SaOS2 and LM7. Paired lines were run side-by-side. β-Actin used as loading control. Error bars represent 95% CI. *P < 0.05.

aged using the EVOS XL Core microscopy system and quantified using Image J.

Stem-cell sphere-forming assay

The sphere-forming assay to assess stem-like ability to re-populate independent of anchorage or attachment was performed by seeding 10^4 cells at a concentration of 10^6 cells/ml onto an ultra-low attachment 6-well plate (Corning) and cultured for up to 7 days, imaging multiple times. The ability to form initial and secondary spheres was assessed using the Image ProPremiere (Media Cybernetics) software suite.

Tail vein in vivo xenograft

In vivo studies were performed in athymic nude mice (nu/nu, Jackson labs). Following trypsinization and inactivation, cells were washed with PBS and re-suspended to a final concentration of 1×10^7 live cells/ml as determined by Countess automated cell counter (Invitrogen). Mice (n=10/cohort) were anesthetized using isofluorane and 100 μL was injected into each nude mouse via the lateral tail vein. Following injection, mice were followed to ensure no adverse effects prevented eating or tasks of daily living. Animal procedures were conducted in compliance with approved IUCUC protocols and in accordance with the principles of animal care set forth by AALAC, as required by Baylor College of Medicine and Texas Children's Hospital (Baylor College of Medicine Animal Protocol AN-5225).

Statistical analysis

Statistical analyses included student's t-test, paired t-test, or ANOVA where applicable. Analyses were performed in Excel and GraphPad Prism. *P* values < 0.05 were considered statistically significant.

Results

To facilitate investigation of mechanisms driving osteosarcoma metastasis, we have previously developed and characterized genetically engineered mouse models (GEMM) of metastatic osteosarcoma [24-27]. Briefly, our model utilized an osteoblast-specific promoter for conditional induction of Cre-recombinase in con-

Table 1. Highlighted differential gene expression in distal metastatic OS

Gene Identifier	Fold-change (Distal Metastasis/ Primary Lesion)
CLDN18	5.059371
MUC1	4.231578
GATA6	3.582778
TACSTD2	3.501185
HDC	3.454002
ALDH1A1	3.36582
ITGB6	3.353894
TGM2	2.838189
UPK1B	2.774326
ICAM1	2.774323
RAB27A	2.758716
GPNMB	2.753676
GRB7	2.685492
CCL6	2.677191
CLDN3	2.647733
ARHGAP8	1.504133
WNT2	1.502982
PDGFC	0.652597
LRRC15	0.534254
CAPN6	0.370261

Paired tissue samples (Primary, Metastasis) extracted from each GEMM mouse. (n=7 pairs) ($P < 0.05$ for all genes shown).

junction with heterozygous or homozygous floxed *Trp53* alleles, or knock-in of a gain-of-function missense p53 [13]. Gene expression profiles from paired primary bone and distal metastatic tumors and established GEMM-derived OS paired cell lines were performed (**Figure 1A**). Comparisons from both paired tissue and paired cell lines identified several genes that were significantly differentially expressed between the primary tumor and distal metastatic disease. These data are publically available at the Gene Expression Omnibus (GEO accession #: GSE43281) [13].

Transglutaminase-2 is significantly elevated in distal metastatic osteosarcoma

Genes with consistently altered expression between primary lesions and their corresponding distal metastases were scored for magnitude of alteration (**Table 1**), compared for statistical significance and investigated for biological relevance. Using this narrowed list based on scoring thresholds, bioinformatic analysis yielded several biologically-relevant pathways germane to metastasis. GSEA, Ingenuity Pathway Analysis, and publically-available databases were used to identify and prioritize genes with potential for metastatic function in key pathways. After validation of cDNA microarray with qPCR analysis, we identified TGM2 as significantly upregulated in distal metastatic osteosarcoma lesions.

Analysis of several samples of paired mouse tumor tissue and cell lines from the primary bone and the distal metastatic sites via qPCR analysis showed marked upregulation of *Tgm2* (**Figure 1B**). We subsequently checked *TGM2* expression levels by qPCR in human OS cell lines, including HOS and SaOS2 that have low metastatic potential, and their respective metastatic counterparts, 143B and LM7 [28, 29]. *TGM2* was significantly upregulated in the metastatic LM7 and 143B lines (**Figure 1C**). Protein levels via Western Blot demonstrated enhanced TGM2 protein expression, which corroborated the qPCR findings (**Figure 1D**). Overall, this data demonstrates through multiple model systems that TGM2 is upregulated in metastatic osteosarcoma.

Knockdown and inhibition of TGM2 in OS decreases proliferation, migration, and invasive potential

To assess the functional significance of TGM2 in OS, we performed loss-of-function studies via knocked down of TGM2 in both mouse (**Figure 2**) and human OS cell lines (**Figure 3**). qPCR analysis confirmed siRNA knockdown of TGM2 expression, compared to controls for mouse and human cell lines (**Figures 2A**, **3A**). Downregulation of TGM2 levels demonstrated decreased proliferation, with both transient and stable knockdown (**Figures 2B**, **3A**). Besides assessing effects on OS proliferation, we investigated the effects of decreased TGM2 levels on osteosarcoma migratory and invasive potential. TGM2 knockdown in both mouse and human OS cells demonstrated significantly reduced migration and decreased invasion in transwell assays (**Figures 2C**, **3B**).

Complementing our molecular studies, we performed small-molecule inhibition of TGM2 with the transglutaminase inhibitor cystamine, which demonstrated similar phenotypes to biological knockdown. Specifically, using paired metastatic murine and human cell lines demonstrated that cystamine preferentially inhibits

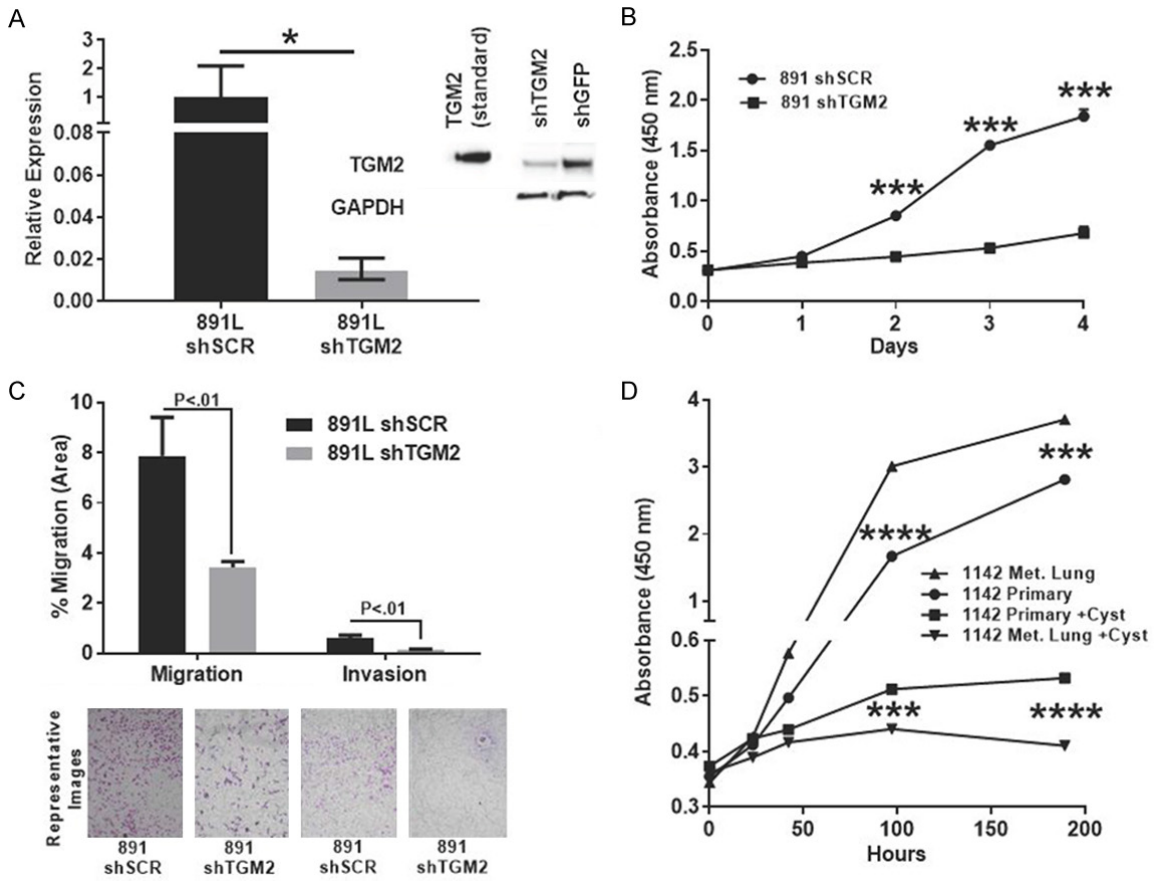

Figure 2. Altered phenotype with TGM2 knockdown in GEMM-derived OS cell line. A: qPCR of TGM2 levels in murine OS following knockdown with either siRNA or shRNA to TGM2. B: Cell proliferation changes resulting from TGM2 knockdown. C: Quantified transwell migration and collagen invasion changes with TGM2 knockdown and representative images. D: Cell proliferation changes resulting from TGM2 inhibition with cystamine for mouse primary and metastatic cell lines. ***P < 0.005.

the proliferation of the high TGM2-expressing, distal metastatic-derived cell lines (**Figures 2D**, **3C**). Furthermore, cystamine also significantly decreased the migratory ability of LM7 cells (**Figure 3D**). Whereas up to this point, the human cell lines displayed congruous results to GEMM mouse lines, we proceeded with human lines to maximize relevance to future translational work.

Overexpression of TGM2 in human cell lines increases metastatic and tumorigenic properties

To demonstrate the corresponding gain-of-function role for TGM2, we stably overexpressed full-length TGM2 in the low-metastatic human OS cell line, SaOS2. Increased TGM2 expression was corroborated by qPCR and Western Blot (**Figure 4A**), which mirrored the parental protein expression differences seen between SaOS2 and LM7. Though TGM2 overexpression did result in a slight increase in proliferative potential, it was not as large a divergence as previously seen with knockdown (**Figure 4B**). Compared to blank vector counterparts, increases in TGM2 enhanced metastatic phenotypes by demonstrating increases in migration and invasion (**Figure 4C**). Further analysis of tumorigenicity, as assessed by soft agar formation in soft agar, demonstrated increased foci with TGM2 overexpression (**Figure 4D**). This demonstrates that TGM2 might not only function in augmenting relocation to the lung from the primary tumor, but also that increased expression of TGM2 within the lung might help foci colonization and progression at that distal site. Overall, both the human and mouse data demonstrate that enhanced TGM2 expression augments metastatic properties in OS and abrogating TGM2 function can reverse these phenotypes.

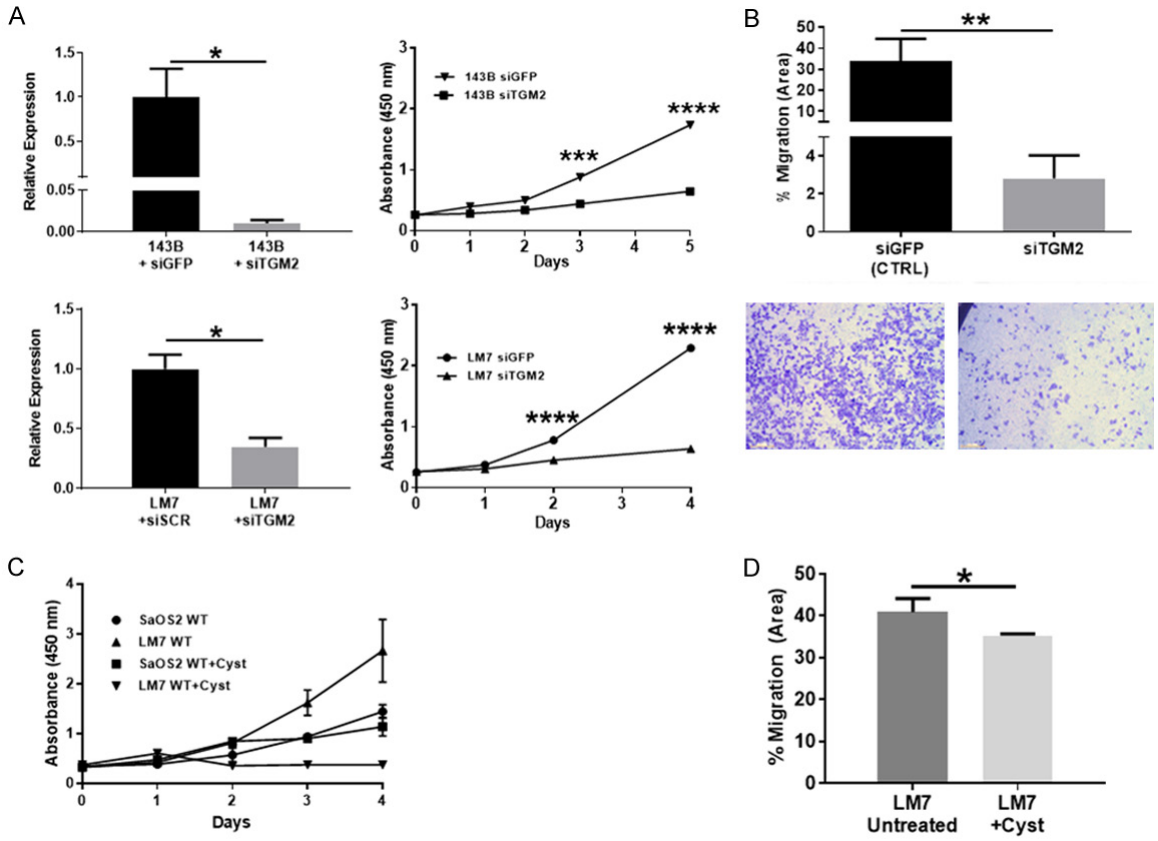

Figure 3. Decreased TGM2 expression or activity inhibits metastatic human OS phenotypes. A: Cell proliferation changes resulting from TGM2 knockdown, as quantified by modified CCK-8 viability assay. qPCR analysis for each cell line is shown adjacent to each respective proliferation assay. B: Quantified transwell migration changes with TGM2 knockdown and representative images. C: Cell proliferation changes resulting from TGM2 inhibition with cystamine, as quantified by modified CCK-8 viability assay for established human OS cell lines with low metastatic (SaOS2) and high metastatic (LM7) properties. D: Effect of cystamine on quantified transwell migration of LM7. Error bars represent 95% CI. *P < 0.05; **P < 0.01; ***P < 0.005; ****P < 0.001.

TGM2 expression enhances stem cell markers and properties

Previous studies in squamous cell carcinoma, breast cancer, glioma, and prostate cancer have demonstrated that TGM2 influences stem cell-like properties, which may be critical for the tumor cell's ability to successfully disseminate and initiate metastatic colonization [23, 30]. To determine if TGM2 expression affects tumor-initiation potential in osteosarcoma, we analyzed the expression of *Nanog*, *OCT4*, *SOX2*, and c-*MYC*, all of which have been identified as or associated with stem cell markers. While c-MYC was not significantly altered (data not shown), the other three stem cell markers were observed to be significantly elevated with increased TGM2 expression (**Figure 5A**).

To further assess stem cell phenotype, we performed a sarcosphere assay. The sarcosphere assay is a surrogate used to evaluate stem cell properties by assessing the ability of the sarcoma cells to form three-dimensional spheres after single cell suspension under low-adherent conditions [31]. Overexpression of TGM2 significantly increased the number of sarcospheres, while knockdown in the metastatic lung cell line LM7 significantly decreased sphere forming capabilities (**Figure 5B**). While TGM2 affected tumor sphere-forming capabilities, size of individual spheres were not significantly altered. These data demonstrate that TGM2 contributes towards OS tumor-initiating properties.

TGM2 knockdown decreases OS metastatic potential in vivo

To investigate the *in vivo* effects of TGM2 on metastatic potential we used the LM7 shTGM2 knockdown stable cell line and performed tail

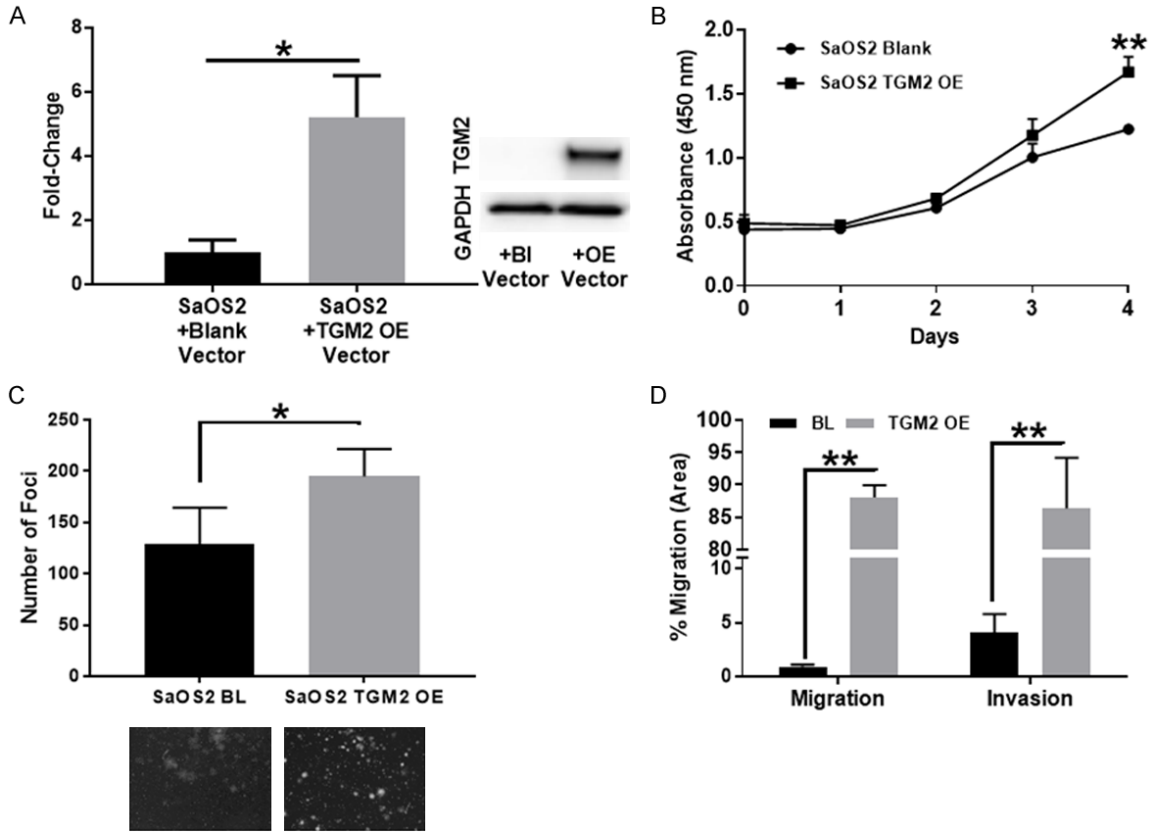

Figure 4. TGM2 overexpression promotes metastatic OS phenotypes. (A) qPCR and WB of TGM2 overexpression in SaOS2. (B) Cell proliferation changes resulting from TGM2 overexpression, as quantified by modified CCK-8 viability assay. Effect of TGM2 overexpression on (C) Quantified soft agar foci formation with representative images below. (D) Quantified transwell migration and invasion through collagen. Error bars represent 95% CI. *P < 0.05; **P < 0.01.

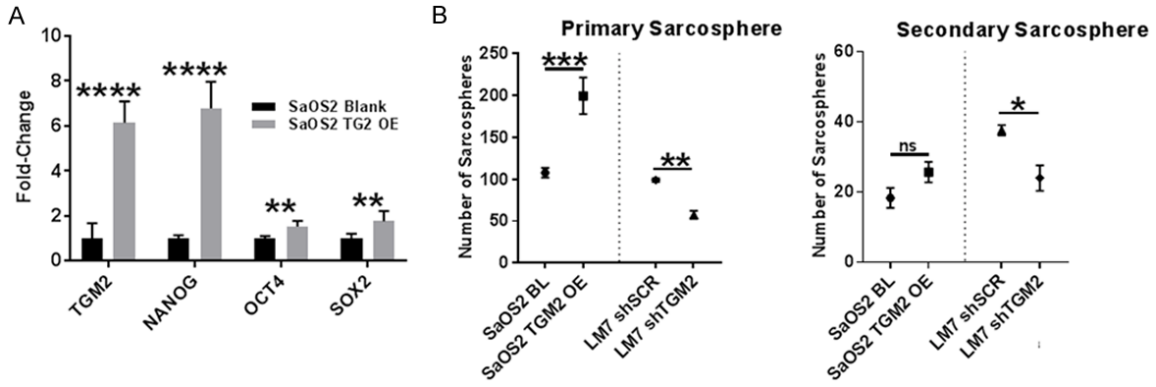

Figure 5. Effect of TGM2 expression on stem cell traits in OS cell lines. A: qPCR of stem-related genes with TGM2 overexpression in SaOS2. B: Effect of altered TGM2 expression on number of primary and secondary sarcospheres. Error bars represent 95% CI. Except with sarcosphere box and whisker plots whiskers show total range (max and min) and box shows interquartile range (25% and 75%). Median line is also shown. **P < 0.01; ***P < 0.005; ****P < 0.001.

vein injection into athymic nude mice. Mice that reached endpoint (death or evidence of disease state incompatible with humane animal care as defined by our IACUC protocol) were subjected immediate necropsy. Subsequently gross metastatic lesions were identified and

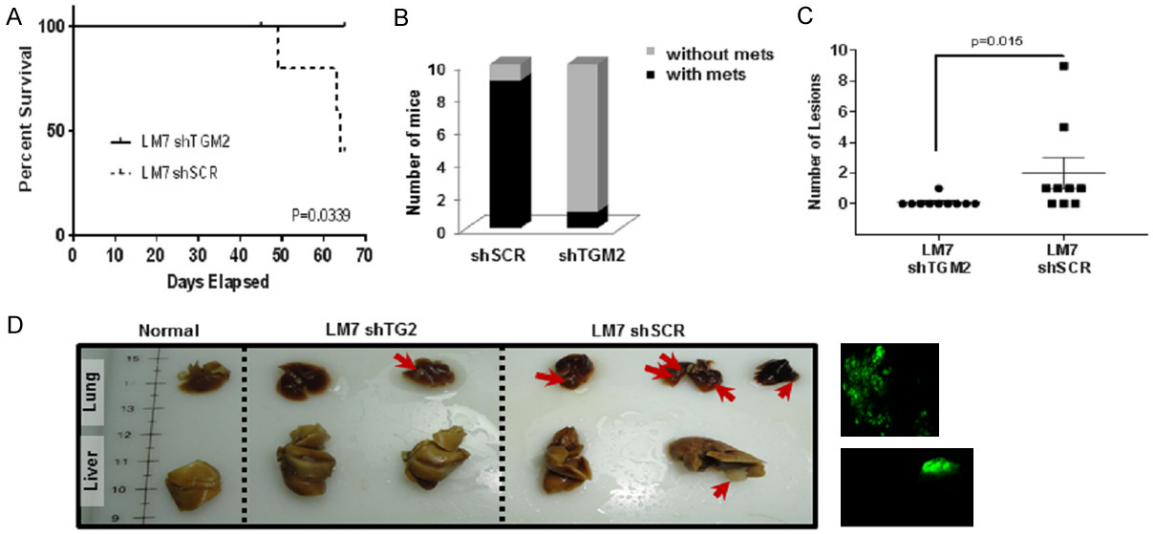

Figure 6. Knockdown of TGM2 prolongs survival and decreases OS metastatic potential *in vivo*. A: Kaplan-Meier survival plot of nude mice following tail vein xenograft of LM7 stable transfected cell lines (shScramble or shTGM2). B: Number of mice with evidence of metastatic disease at time of death. C: Number of gross macroscopic lesions per mouse at time of death. D: Representative lung and liver images of gross lesions and fluorescence (GFP).

quantified. All animals that did not reach endpoint were sacrificed by nine weeks and subjected to necropsy. We observed the vector control cohort demonstrated significantly worse overall survival compared to TGM2 knockdown cohort (**Figure 6A**). At the time of sacrifice, a comprehensive necropsy of the mice demonstrated more widespread parenchymal disease in control LM7 injected mice compared to those injected with TGM2 knockdown cells (**Figure 6B-D**), which could be verified by direct GFP visualization of labeled OS cells (**Figure 6D**). Overall, our findings provide strong evidence that TGM2 significantly contributes to the aggressive nature and metastatic potential for osteosarcoma.

Discussion

Metastatic disease is an imperative cancer characteristic to investigate and treat, as approximately 90% of cancer-related deaths are secondary to the successful dissemination of tumor cells [12, 32]. However, minimal progress has been made over the past several decades towards improving long-term outcomes for patients with metastatic disease.

Osteosarcoma is a highly aggressive mesenchymal malignancy with long term outcomes of less than 25% survival for patients with metastatic disease. Unfortunately, it is extremely difficult to obtain pre-treated, chemotherapy-naïve metastatic tumors, which further complicates our ability to understand the molecular traits of metastatic disease at time of diagnosis. Thus, use of innovative model systems that mimic the spontaneous initiation and progression of OS have the ability to provide essential insights into the molecular pathogenesis of the metastatic disease.

Comprehensive molecular analysis of these spontaneous models allowed for the identification of genetic perturbations associated with metastatic osteosarcoma. Specifically, one perturbation we identified was enhanced expression of TGM2 in the distal lung and liver metastatic lesions. When it was first brought to the forefront as a prognostic antigen for celiac disease, several mechanisms of action corresponding to inflammation and immune response were identified as biologically relevant to disease progression [15, 16, 18, 33]. More recently, these functions are being investigated in tumorigenesis and cancer, with less common functions being discovered. These include acting as a signaling molecule, scaffolding protein, and transcriptional enhancer [23, 33]. Downstream targets and pathways of TGM2 are actively being investigated and may include PTEN, integrin-mediated signaling pathways, TGF-β networks and many other pro-metastatic or pro-motility roles [30, 33-35]. An additional aspect is the influence TGM2 may

have in the metastatic process by enzymatically altering the extracellular matrix (ECM). This is particularly intriguing, given recent studies in OS and other cancers linking ECM components such as fibulins, fibrillins, proteoglycans and TGM2 [36-39].

Our studies provide significant evidence that TGM2 contributes to metastatic phenotypes for OS, including enhancing invasive potential. Interestingly, we also observed that TGM2 can enhance molecular and physical features associated with stem cell properties and have preliminary evidence that TGM2 can further enhance mesenchymal stem cell signatures. While TGM2 enhances metastatic and stem-like properties in OS, further detailed studies are necessary to determine additional molecular mechanisms underlying these contributions secondary to perturbations in TGM2.

Our *in vivo* results indicate that TGM2 expression significantly contributes to the establishment of metastatic lesions in the lung, independent of any benefit that might be present in escaping the primary tumor site. This is clear, because when we eliminate the invasive step and introduce the cells via tail vein injection, we see decreased metastases with TGM2 knockdown. In addition, due to the previously reported enzymatic functions of TGM2, we are actively interested in pursuing how alterations in TGM2 levels, and subsequent activity, can potentially dictate the interactions required for successful establishment of metastatic lesions within the distal metastatic tissues. Specifically, we are investigating how TGM2 levels can influence the three-dimensional interactions between the sarcoma cells and lung parenchyma. Using co-culture experiments with OS cell and lung fibroblast-specific fluorescent labeling we are investigating the effects of TGM2 expression on nodule formation. Such studies could provide additional insights into whether inhibition of TGM2 can specifically disrupt metastatic foci formation and/or integrity.

Our investigation into small molecule inhibitors of TGM2 was not exhaustive, given the large number of non-specific transglutaminase and TGM2-specific inhibitors available. However, it does provide valuable insights into the possibility that targeting TGM2 activity could diminish the metastatic potential for osteosarcoma. Though cystamine was quite effective at inhibiting several of the metastatic properties associated with TGM2, further investigation into more specific TGM2 inhibitors could yield significant advances in treating the disease clinically. It is particularly interesting that throughout our studies, cells with increased levels of TGM2 (WT vs. knockdown or OE vs. blank) were more sensitive to the cystamine. A TGM2 inhibitor that augments treatment specifically in metastatic lesions that harbor stem-like cells would be a significant advancement in treating metastatic OS.

Acknowledgements

This work was supported by funding from Cancer Prevention Research Institute of Texas (RP140022-C2) (JTY), Sarcoma Foundation of America (JTY) and St. Baldrick's Foundation (JTY).

Disclosure of conflict of interest

None.

Address correspondence to: Dr. Jason T Yustein, Texas Children's Cancer and Hematology Centers and The Faris D. Virani Ewing Sarcoma Center, Baylor College of Medicine, 1102 Bates St., Suite 1025.07, Houston 77030, Texas, USA. Tel: 832-824-4601; Fax: 832-825-4846; E-mail: yustein@bcm.edu

References

[1] Velletri T, Xie N, Wang Y, Huang Y, Yang Q, Chen X, Chen Q, Shou P, Gan Y, Cao G, Melino G and Shi Y. P53 functional abnormality in mesenchymal stem cells promotes osteosarcoma development. Cell Death Dis 2016; 7: e2015.

[2] Abarrategi A, Tornin J, Lucia MC, Hamilton A, Enrique MC, Rodrigo JP, González MV, Baldini N, Javier GC and Rodriguez R. Osteosarcoma: cells-of-origin, cancer stem cells, and targeted therapies. Stem Cells International 2016; 2016: 3631764.

[3] Kansara M, Teng MW, Smyth MJ and Thomas DM. Translational biology of osteosarcoma. Nat Rev Cancer 2014; 14: 722-735.

[4] Mutsaers AJ and Walkley CR. Cells of origin in osteosarcoma: mesenchymal stem cells or osteoblast committed cells? Bone 2014; 62: 56-63.

[5] Bousquet M, Gibrat C, Ouellet M, Rouillard C, Calon F and Cicchetti F. Cystamine metabolism and brain transport properties: clinical implications for neurodegenerative diseases. J Neurochem 2010; 114: 1651-1658.

[6] Isakoff MS, Bielack SS, Meltzer P and Gorlick R. Osteosarcoma: current treatment and a collaborative pathway to success. J Clin Oncol 2015; 33: 3029-3035.
[7] Ries LA, Melbert D, Krapcho M, Stinchcomb DGHN, Horner MJ, Mariotto A, Miller BA, Feuer EJ, Altekruse SF, Lewis DR, Clegg L, Eisner MP, Reichman M and Edwards BK. SEER cancer statistics review, 1975-2005, National Cancer Institute. Bethesda, MD, http://seer.cancer.gov/csr/1975_2005/, based on November 2007 SEER data submission, posted to the SEER web site, 2008. http://seer.cancer.gov/csr/1975_2012/2008; 1-101.
[8] Siegel RL, Miller KD and Jemal A. Cancer statistics, 2016. CA Cancer J Clin 2016; 66: 7-30.
[9] Walters DK, Steinmann P, Langsam B, Schmutz S, Born W and Fuchs B. Identification of potential chemoresistance genes in osteosarcoma. Anticancer Res 2008; 28: 673-679.
[10] Osasan S, Zhang M, Shen F, Paul PJ, Persad S and Sergi C. Osteogenic sarcoma: a 21st century review. Anticancer Res 2016; 36: 4391-4398.
[11] Botter SM, Neri D and Fuchs B. Recent advances in osteosarcoma. Curr Opin Pharmacol 2014; 16: 15-23.
[12] Ham SJ, Schraffordt Koops H, van der Graaf WT, van Horn JR, Postma L and Hoekstra HJ. Historical, current and future aspects of osteosarcoma treatment. Eur J Surg Oncol 1998; 24: 584-600.
[13] Zhao S, Kurenbekova L, Gao Y, Roos A, Creighton CJ, Rao P, Hicks J, Man TK, Lau C, Brown AM, Jones SN, Lazar AJ, Ingram D, Lev D, Donehower LA and Yustein JT. NKD2, a negative regulator of Wnt signaling, suppresses tumor growth and metastasis in osteosarcoma. Oncogene 2015; 34: 5069-5079.
[14] Chen X, Hnida K, Graewert MA, Andersen JT, Iversen R, Tuukkanen A, Svergun D and Sollid LM. Structural basis for antigen recognition by transglutaminase 2-specific autoantibodies in celiac disease. J Biol Chem 2015; 290: 21365-21375.
[15] Iversen R, Fleur du Pre M, Di Niro R and Sollid LM. Igs as substrates for transglutaminase 2: implications for autoantibody production in celiac disease. J Immunol 2015; 195: 5159-5168.
[16] Rauhavirta T, Hietikko M, Salmi T and Lindfors K. Transglutaminase 2 and transglutaminase 2 autoantibodies in celiac disease: a review. Clin Rev Allergy Immunol 2016; [Epub ahead of print].
[17] He W, Sun Z and Liu Z. Silencing of TGM2 reverses epithelial to mesenchymal transition and modulates the chemosensitivity of breast cancer to docetaxel. Exp Ther Med 2015; 10: 1413-1418.
[18] Huang L, Xu AM and Liu W. Transglutaminase 2 in cancer. Am J Cancer Res 2015; 5: 2756-2776.
[19] Lee J, Condello S, Yakubov B, Emerson R, Caperell-Grant A, Hitomi K, Xie J and Matei D. Tissue transglutaminase mediated tumor-stroma interaction promotes pancreatic cancer progression. Clin Cancer Res 2015; 21: 4482-4493.
[20] Min B, Park H, Lee S, Li Y, Choi JM, Lee JY, Kim J, Choi YD, Kwon YG, Lee HW, Bae SC, Yun CO and Chung KC. CHIP-mediated degradation of transglutaminase 2 negatively regulates tumor growth and angiogenesis in renal cancer. Oncogene 2016; 35: 3718-3728.
[21] Wang X, Yu Z, Zhou Q, Wu X, Chen X, Li J, Zhu Z, Liu B and Su L. Tissue transglutaminase-2 promotes gastric cancer progression via the ERK1/2 pathway. Oncotarget 2016; 7: 7066-7079.
[22] Yu C, Cao Q, Chen P, Yang S, Gong X, Deng M, Ruan B and Li L. Tissue transglutaminase 2 exerts a tumor-promoting role in hepatitis B virus-related hepatocellular carcinoma. Tumor Biol 2016; [Epub ahead of print].
[23] Eckert RL, Fisher ML, Grun D, Adhikary G, Xu W and Kerr C. Transglutaminase is a tumor cell and cancer stem cell survival factor. Mol Carcinog 2015; 54: 947-958.
[24] Allen-Rhoades W, Kurenbekova L, Satterfield L, Parikh N, Fuja D, Shuck RL, Rainusso N, Trucco M, Barkauskas DA, Jo E, Ahern C, Hilsenbeck S, Donehower LA and Yustein JT. Cross-species identification of a plasma microRNA signature for detection, therapeutic monitoring, and prognosis in osteosarcoma. Cancer Med 2015; 4: 977-988.
[25] Donehower LA. Using mice to examine p53 functions in cancer, aging, and longevity. Cold Spring Harb Perspect Biol 2009; 1: a001081.
[26] Donehower LA and Lozano G. 20 years studying P53 functions in genetically engineered mice. Nat Rev Cancer 2009; 9: 831-841.
[27] Rao PH, Zhao S, Zhao YJ, Yu A, Rainusso N, Trucco M, Allen-Rhoades W, Satterfield L, Fuja D, Borra VJ, Man TK, Donehower LA and Yustein JT. Coamplification of Myc/Pvt1 and homozygous deletion of Nlrp1 locus are frequent genetics changes in mouse osteosarcoma. Genes Chromosomes Cancer 2015; 54: 796-808.
[28] Duan X, Jia SF, Zhou Z, Langley RR, Bolontrade MF and Kleinerman ES. Association of alphavbeta3 integrin expression with the metastatic potential and migratory and chemotactic ability of human osteosarcoma cells. Clin Exp Metastasis 2004; 21: 747-753.

[29] Luu HH, Kang Q, Park JK, Si W, Luo Q, Jiang W, Yin H, Montag AG, Simon MA, Peabody TD, Haydon RC, Rinker-Schaeffer CW and He TC. An orthotopic model of human osteosarcoma growth and spontaneous pulmonary metastasis. Clin Exp Metastasis 2005; 22: 319-329.
[30] Fisher ML, Adhikary G, Xu W, Kerr C, Keillor JW and Eckert RL. Type II transglutaminase stimulates epidermal cancer stem cell epithelial-mesenchymal transition. Oncotarget 2015; 6: 20525-20539.
[31] Rainusso N, Man TK, Lau CC, Hicks J, Shen JJ, Yu A, Wang LL and Rosen JM. Identification and gene expression profiling of tumor-initiating cells isolated from human osteosarcoma cell lines in an orthotopic mouse model. Cancer Biol Ther 2011; 12: 278-287.
[32] Hanahan D and Weinberg RA. Hallmarks of cancer: The next generation. Cell 2011; 144: 646-674.
[33] Nurminskaya MV and Belkin AM. Cellular functions of tissue transglutaminase. Int Rev Cell Mol Biol 2012; 294: 1-97.
[34] Agnihotri N and Mehta K. Transglutaminase-2: evolution from pedestrian protein to a promising therapeutic target. Amino Acids 2017; 49: 425-439.
[35] Burhan I, Furini G, Lortat-Jacob H, Atobatele AG, Scarpellini A, Schroeder N, Atkinson J, Maamra M, Nutter FH, Watson P, Vinciguerra M, Johnson TS and Verderio EA. Interplay between transglutaminases and heparan sulphate in progressive renal scarring. Sci Rep 2016; 6: 31343-31343.
[36] Freeman LJ, Lomas A, Hodson N, Sherratt MJ, Mellody KT, Weiss AS, Shuttleworth A, Kielty CM. Fibulin-5 interacts with fibrillin-1 molecules and microfibrils. Biochem J 2005; 388: 1-5.
[37] Kielty CM, Sherratt MJ and Shuttleworth CA. Elastic fibres. J Cell Sci 2002; 115: 2817-2828.
[38] Robertson I, Jensen S and Handford P. TB domain proteins: evolutionary insights into the multifaceted roles of fibrillins and LTBPs. Biochem J 2011; 433: 263-276.
[39] Wang S, Zhang D, Han S, Gao P, Liu C, Li J and Pan X. Fibulin-3 promotes osteosarcoma invasion and metastasis by inducing epithelial to mesenchymal transition and activating the Wnt/β-catenin signaling pathway. Sci Rep 2017; 7: 6215-6215.